PHYSICAL REVIEW A **85**, 031402(R) (2012)

Coherent control of collective atom phase for ultralong, inversion-free photon echoes

Byoung S. Ham*

Center for Photon Information Processing, School of Electrical Engineering, Inha University, 253 Yonghyun-dong, Nam-gu, Incheon 402-751, South Korea

(Received 18 October 2011; published 27 March 2012)

To overcome the fundamental limitations of the π optical pulse-induced population inversion and optical decay-caused short storage time in conventional photon echoes, a coherent control of collective atoms is studied for inversion-free, optical decay-halted photon echoes, where the constraint of photon storage time is now replaced by a spin population decay process. Using phase-controlled double rephasing, an inversion-free photon echo scheme is obtained, where no spontaneous or stimulated emission-driven quantum noise exists. Thus, the present method can be applied for ultralong quantum memories in quantum repeaters for long-distance quantum communications.

DOI: 10.1103/PhysRevA.85.031402 PACS number(s): 42.50.Md, 82.53.Kp

Over the past decade, quantum information processing has been widely investigated for potential applications in quantum computing and quantum communications. To overcome a limited transmission distance through an optical fiber, quantum communications beyond 100 km have been an ultimate goal. Using quantum repeaters [1], the limited transmission distance can be greatly extended, as with optical amplifiers in present fiber-optic networks. In this case, ultralong quantum memory is essential, where the minimum storage time for global quantum communications is about 1 s [2].

Photon echoes have been intensively studied for all-optical information processing owing to their wide bandwidth, fast access time, and multimode capabilities in both time and space domains [3,4]. Photon echoes are based on the reversibility of inhomogeneously broadened atom (or spin) phases, where the reversible atom phase is obtained by an optical π pulse-caused population swapping between two states, resulting in population inversion. For quantum memory applications, however, conventional photon echoes following two-pulse [3] or three-pulse schemes [4] have been excluded due mainly to quantum noise from the rephasing-caused population inversion. Obtaining a phase decay time that is much longer than a millisecond is another goal for quantum memories. Although solid media have no atomic diffusion and pose a longer phase decay time compared with atomic vapors [5], the observed photon storage time in several modified schemes is still too short to apply it for long-distance quantum communications [6–12].

Recently a double-rephasing method for conventional two-pulse photon echoes [13] has been analyzed for a quantum memory scheme by using the concept of silent echo [14]. However, the storage time is still limited by optical phase decay time. Here, an ultralong, inversion-free photon echo scheme is proposed using double rephasing [13], combined with optical locking in three-pulse photon echoes (3PE) [15], where the optical locking is originally proposed in resonant Raman echoes [16]. In this case, both phase-locked atoms as inherent properties of 3PE [4] and controlling atom phases for the optical-spin coherence transfer play a key role [10–13,15,16].

In Fig. 1, an inhomogeneously broadened Λ-type three-level optical system is considered, where D (data), W (write), R (read), and RR (re-rephasing) pulses are resonant for the transition of $|1\rangle$ (ground) to $|3\rangle$ (excited). The optical locking pulses $C1$ and $C2$ are resonant to the transition of $|2\rangle$-$|3\rangle$ for coherent population transfer, where $|2\rangle$ is an auxiliary ground state [10,12]. Because the spin decay rates for the $|1\rangle$-$|2\rangle$ transition are robust compared with their optical counterparts ($|1\rangle$-$|3\rangle$ and $|2\rangle$-$|3\rangle$), $C1$ functions as a storage time extension due to optical decay halt [12,15]. Unlike two-pulse photon echoes [3], the photon storage time extension by $C1$ in Fig. 1 is independent of optical phase decay as well as spin phase decay due to intrinsic atom phase locking in the 3PE (discussed in Fig. 2) [15].

The inset of Fig. 1(a) shows a corresponding pulse sequence, where D, W, and R satisfy a conventional 3PE scheme. The pulse area of R ($\Phi_R = 3\pi/2$), however, increases threefold over the conventional one ($\Phi_R = \pi/2$) to satisfy the phase recovery condition for optical locking by $C1$ and $C2$ (discussed in Figs. 3 and 4). Thus, the three-pulse photon echo $E1$ in Figs. 1(a) and 1(b) becomes absorptive (or negative) in coherence, where stimulated emission (as a major noise factor to quantum memories [17]) by $E1$ must be quenched. However, the coherent absorption by $E1$ may alter the quantum fidelity of $E2$. This $E1$ induced-absorption problem can be solved easily by using a spatial phase-mismatching condition.

Let us consider an angled scheme for Fig. 1(a), where a counterpropagating beam set of D and RR has a small angle with another counterpropagating beam set of W and $R1$: $\mathbf{k}_D = -\mathbf{k}_{RR}$, $\mathbf{k}_W = -\mathbf{k}_R$, where $\mathbf{k}_i$ is a propagation wave vector of each pulse i. Then, the phase-matching directions for $E1$ and $E2$ are, respectively,

$$\mathbf{k}_{E1} = \mathbf{k}_R + \mathbf{k}_W - \mathbf{k}_D = -\mathbf{k}_D, \tag{1}$$

$$\mathbf{k}_{E2} = 2\mathbf{k}_{RR} - \mathbf{k}_{E1} = 2\mathbf{k}_{RR} + \mathbf{k}_D - (\mathbf{k}_R + \mathbf{k}_W) = -\mathbf{k}_D. \tag{2}$$

Unlike the spatial phase mismatch for $E1$ along the medium length L ($L \gg \lambda$) due to $|\mathbf{k}_{E1} - \mathbf{k}_D| = 2k_D L \gg$

*bham@inha.ac.kr

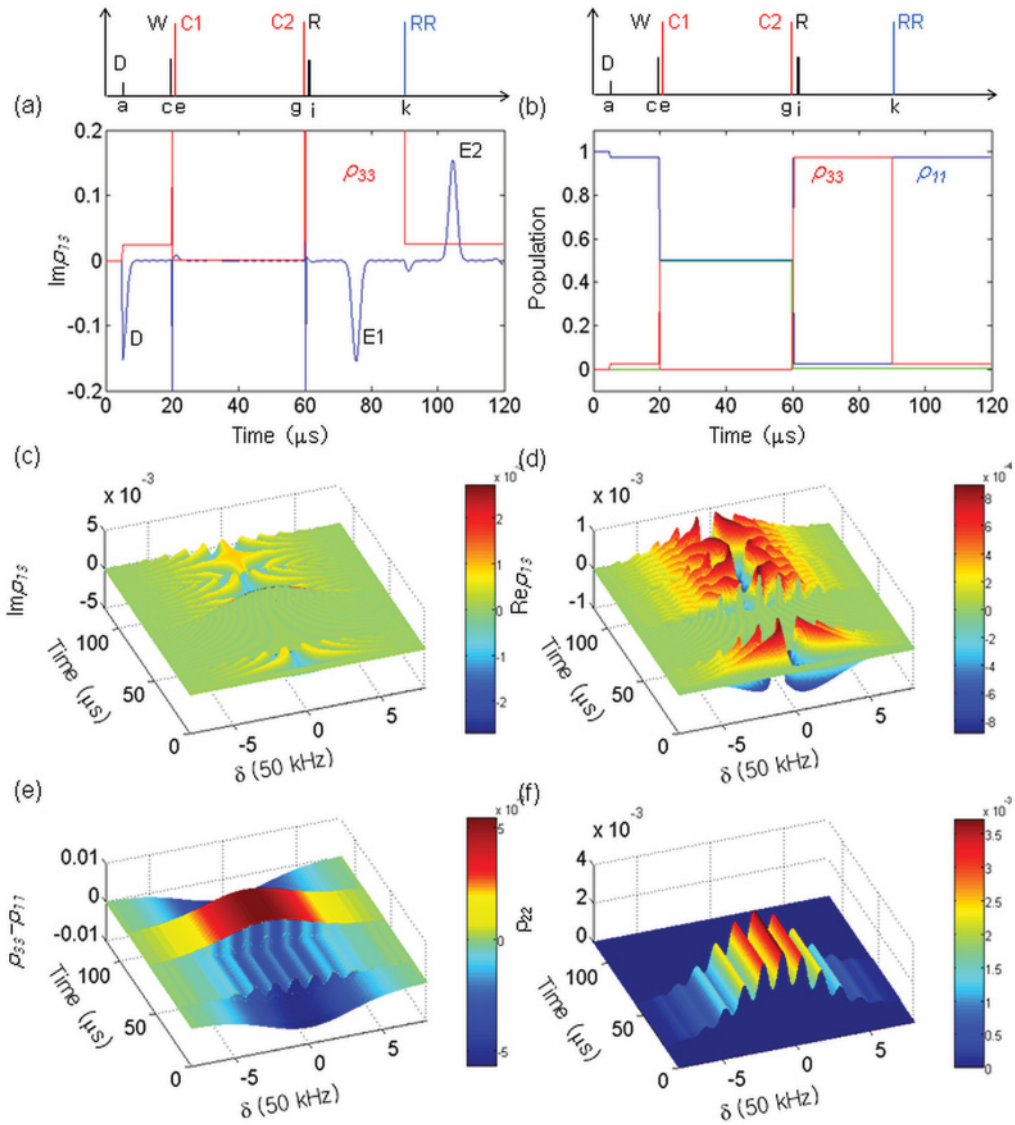

FIG. 1. (Color online) Inversion-free storage time extended photon echo. (a) and (b) Optical coherence and population as a function of time, respectively. The pulse area of D, W, R, and RR is 0.1π, 0.5π, 1.5π, and π, respectively. Each pulse area of $C1$ and $C2$ is π. Inset: Pulse sequence. (a) $T_D = 5.0$; (c) $T_W = 20.0$; (e) $T_{C1} = 20.1$; (g) $T_{C2} = 60.0$; (i) $T_R = 60.1$; (k) $T_{RR} = 90.0$ μs. Green (light gray): ρ_{22}; red (gray): ρ_{33}. (c)–(f) Coherence evolution for all atoms as a function of detuning and time. The optical inhomogeneous width [full width at half maximum (FWHM)] is 340 kHz. Each pulse duration is 100 ns except for D and R. The D pulse area is 0.1π. All decay parameters are set to zero.

π in Eq. (1) resulting in a silent echo [14], echo $E2$ stays in phase due to $\mathbf{k}_{E2} - \mathbf{k}_{E1} = 0$ in Eq. (2). Here, the silent echo $E1$ does not affect the individual atom's phase evolution, and thus echo $E2$ as a two-pulse echo of $E1$ results from these individual atoms' rephasing process by RR.

Figures 1(c)–1(f) show coherence evolutions of all excited atoms. In Figs. 1(c) and 1(e), the echo $E2$ at $t = 105$ μs is without population inversion, while the (absorptive or negative) echo $E1$ at $t = 75$ μs is with population inversion. The storage time extension is due to the population transfer by $C1$ to the spin state $|2\rangle$ [10–13], where atom phase locking resulting from the W pulse is still effective for spin transitions (discussed in Fig. 2), even under spin inhomogeneous broadening, as experimentally demonstrated [15].

For the calculations, nine time-dependent density matrix equations are numerically solved for an 800-kHz inhomogeneously broadened Gaussian-distributed atom ensemble. For visualization purposes, all decay rates are set at zero. Because the pulse duration of the *data* pulse D is as short as the inverse of the inhomogeneous broadening, the delay time of the *write* pulse W from D can also be kept short enough as compared with the optical phase decay time for nearly maximum coherence.

In Figs. 2 and 3, we discuss how the phase-locked atoms play an important role via optical-spin coherence transfer for storage time extension. We also discuss collective atom phase control in the optical locking processes by using extra rephasing. In Fig. 2, all figures are color matched. The blue (dark gray) and red (gray) curves in Fig. 2(a) indicate

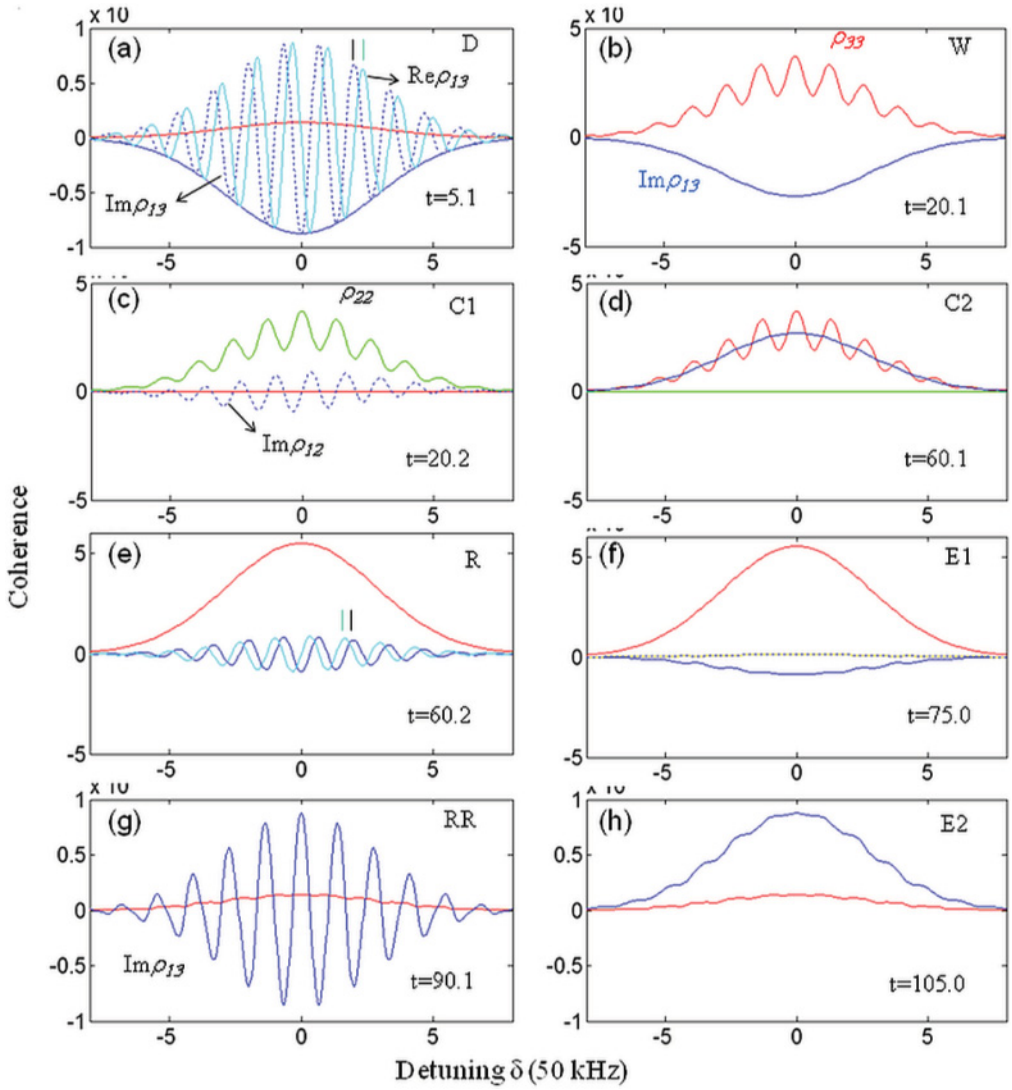

FIG. 2. (Color online) Coherence vs detuning for Fig. 1. (a) $t = 5.1\ \mu$s for D excitation in the 0.1π pulse area (see blue and red curves; For $t = 20.0\ \mu$s just before W, see cyan and dotted modulation curves). (b) $t = 20.1\ \mu$s for W excitation in the $\pi/2$ pulse area. (c) $t = 20.2\ \mu$s for $C1$ (π pulse area). (d) $t = 60.1\ \mu$s for $C2$ (π pulse area). (e) R rephasing with the $3\pi/2$ pulse area. (f) Silent echo $E1$ at $t = 75\ \mu$s. (g) RR rephasing with a π pulse area. (h) Inversion-free echo $E2$ at $t = 105\ \mu$s. Blue (dark gray): Imρ_{13}; red (gray): ρ_{33}; green (light gray): ρ_{22}; cyan (medium gray): Reρ_{13}.

D-pulse-excited coherence (Imρ_{13}) and population (ρ_{33}) in a spectral domain at $t = 5.1\ \mu$s, respectively. Defining δ^ι as a detuning of an atom group ι from the line center in the inhomogeneously broadened ensemble, each δ-detuned atom ι evolves at a different speed $[\rho_{13}^\iota(t + t_0)\exp(\pm i\delta^\iota t)$; t_0 indicates the ending time of an excitation pulse; see also Figs. 1(c) and 1(d)], resulting in a phase modulation as shown in the dotted curve, Imρ_{13} for $t = 20.0\ \mu$s just before the W pulse is turned on. The cyan (medium gray) curve is for the corresponding real part, Reρ_{13}, which is $\pi/2$ phase shifted. The optical information about the data pulse D is stored in this time-dependent optical phase modulation, i.e., atom phase grating: This is the storage mechanism of two-pulse photon echoes. As rephasing-based photon echoes are satisfied for quantum memories [6–9], the 3PE should also be satisfied, if the optical population decay-caused coherence loss is ignored [7,8].

The 3PE scheme is obtained from the two-pulse photon echo scheme composed of D and R' at a π pulse area [3], by simply dividing the R' into two halves, W and R [4]. In Fig. 2(b), a half π pulse (W) excites only half of each population in each state, resulting in a population grating for both ρ_{11} (not shown) and ρ_{33} (red/gray curve). This population grating ρ_{33} is coherently transferred by W from the phase grating, Imρ_{13} (see also the bottom row of Fig. 3). At this stage, the system coherence becomes locked from the phase decay process, resulting in atom phase locking. This phase locking is an ultimate property of the 3PE [4].

Subsequently, the π pulse $C1$ that follows then coherently transfers the population grating ρ_{33} into the spin state $|2\rangle$ to halt optical population decay-caused decoherence: See the exact same pattern between ρ_{22} (green/light gray) and ρ_{33} in Figs. 2(b) and 2(c). Via this complete population transfer, optical coherence is also transferred into spin coherence (see

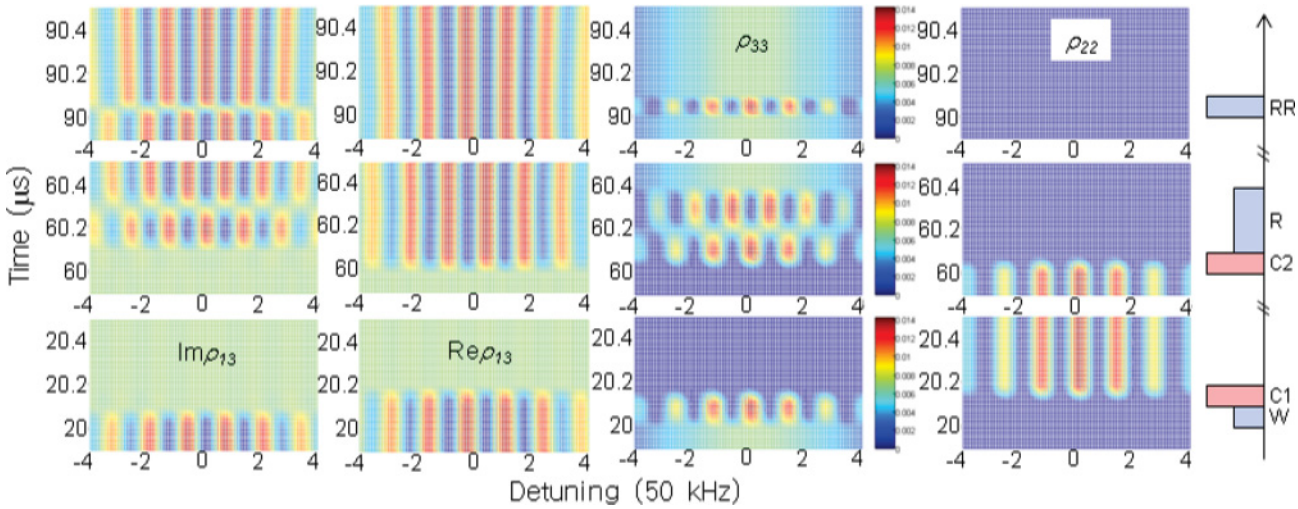

FIG. 3. (Color online) Detailed coherence change by each pulse interaction as a function of time and detuning. All the parameters are the same as those in Fig. 1, except the pulse area of D.

the dotted curve for Imρ_{12}). As the optical coherence (ρ_{13}) is phase locked by W, the spin coherence (ρ_{12}) is also phase locked [15]: Compare this with the spin-dephasing-dependent decoherence in two-pulse echoes [11,12]. In Fig. 2(d), by the $C2$ pulse, the transferred atoms are returned to state $|3\rangle$, recovering both optical population and coherence. However, a π phase shift results [see the inverted blue/dark gray curve compared with that of Fig. 2(b)].

As shown in Fig. 2(e), by R at $t = 60.2$ μs, the modulation in ρ_{33} (red/gray) in Fig. 2(b) is transferred back into the phase grating (Imρ_{13}; blue/dark gray), and rephasing of coherence begins. Here, the $3\pi/2$ *read* pulse R is used to compensate the optical locking pulse-induced π phase shift [10,11]. The rephased coherence as an echo $E1$ in Fig. 2(f), however, is absorptive (see the blue/dark gray) with population inversion (red/gray), resulting in a silent echo in an angled counterpropagating scheme as discussed in Fig. 1. This absorptive echo property was anticipated in Fig. 2(e), where no phase change occurs in absorption, Imρ_{13}.

By the *re-rephasing* pulse RR at $t = 90.0$ μs, $E2$ results from $E1$ [see Figs. 2(g) and 2(h)]. Because RR functions as two-pulse photon echoes [3], the system undergoes no population inversion. Thus, echo $E2$ in Fig. 2(h) is free from both spontaneous and stimulated emission processes. The wiggles in Figs. 2(f) and 2(h) are due to δ-dependent imperfect rephasing in the simulations.

Figure 3 shows details of collective atom phase control. For maximum coherence excitation, a $\pi/2$ pulse area of D is used. The corresponding pulse sequence is the same as in Fig. 1 (see the far right-hand column). As shown in the bottom row, the *write* pulse W functions as the coherence transfer from the phase grating (ρ_{13}) to the population grating [ρ_{33} as well as ρ_{11} (not shown)] as discussed in Fig. 2. This population grating has nothing to do with the optical phase decay as discussed in Fig. 2(b). The optical locking pulse $C1$ results in coherence transfer from the optical state (ρ_{33}) to the spin state (ρ_{22}) via the population transfer as discussed in Fig. 2(c): See the two right-hand columns. Because the transferred atoms are phase locked, spin coherence can continue as long as ρ_{22} decays out.

In the middle row of Fig. 3, the spin population in state $|2\rangle$ is returned to state $|3\rangle$ by $C2$. During this process by $C1$ and $C2$, a total π phase shift occurs (see the color swapping in both Imρ_{13} and Reρ_{13} compared with the bottom row). At the end of the $3\pi/2$ R pulse, however, the optical coherence Imρ_{13} has the same phase as that by D, which is absorptive or negative (see the first column) under population inversion.

The RR pulse-resulted echo $E2$ is the exact coherence retrieval of $E1$ in the context of a conventional two-pulse photon echo, where $E1$ is silent in a counterpropagating angled scheme. This fact also leads to an important conclusion that the retrieval order of the inversion-free echo $E2$ is the same as that of data D [see Fig. 4(e)].

In Fig. 4, the atom phase control discussed in Figs. 1–3 is speculated on by using a Bloch vector model. Figure 4(a) shows the coherence evolution of a detuned atom group at $\delta =$ 10 kHz, where coherence evolution [Figs. 4(b) and 4(c)] is retrieved by RR.

Figure 4(b) represents a Bloch model for Fig. 4(a). The D-excited atomic coherence at point b is retrieved by R, resulting in photon echo $E1$ at the bottom of the figure very near point b. The coherence of echo $E1$, however, is negative and silent under the population inversion [see Fig. 1(a)]. By the additional rephasing pulse RR, echo $E2$ results from echo $E1$ (see the $\times$ mark on the top curve), without population inversion, as discussed in Figs. 1(a) and 2(h).

Figures 4(c) and 4(d) represent the atom phase control by R to support the phase recovery condition. As shown in Fig. 4(d), for a complete retrieval of $E1$, the π pulse area of R (blue/dark gray shaded region between points x and y) must be added to give a π phase shift in total. As discussed in Fig. 3, where $C1$ and $C2$ result in a π phase shift to ρ_{13}, the value of Imρ_{13} and Reρ_{13} at point x must be opposite to that at point c: $\rho_{13}(t + t_0)\exp(i\delta t)$ at $c \rightarrow -\rho_{13}(t + t_1)\exp(i\delta t)$ at x. This condition represents negative absorption under the population inversion [see Fig. 4(e)].

In Fig. 4(e) the present inversion-free photon echo scheme is described for multiple data pulses. As shown, the order of

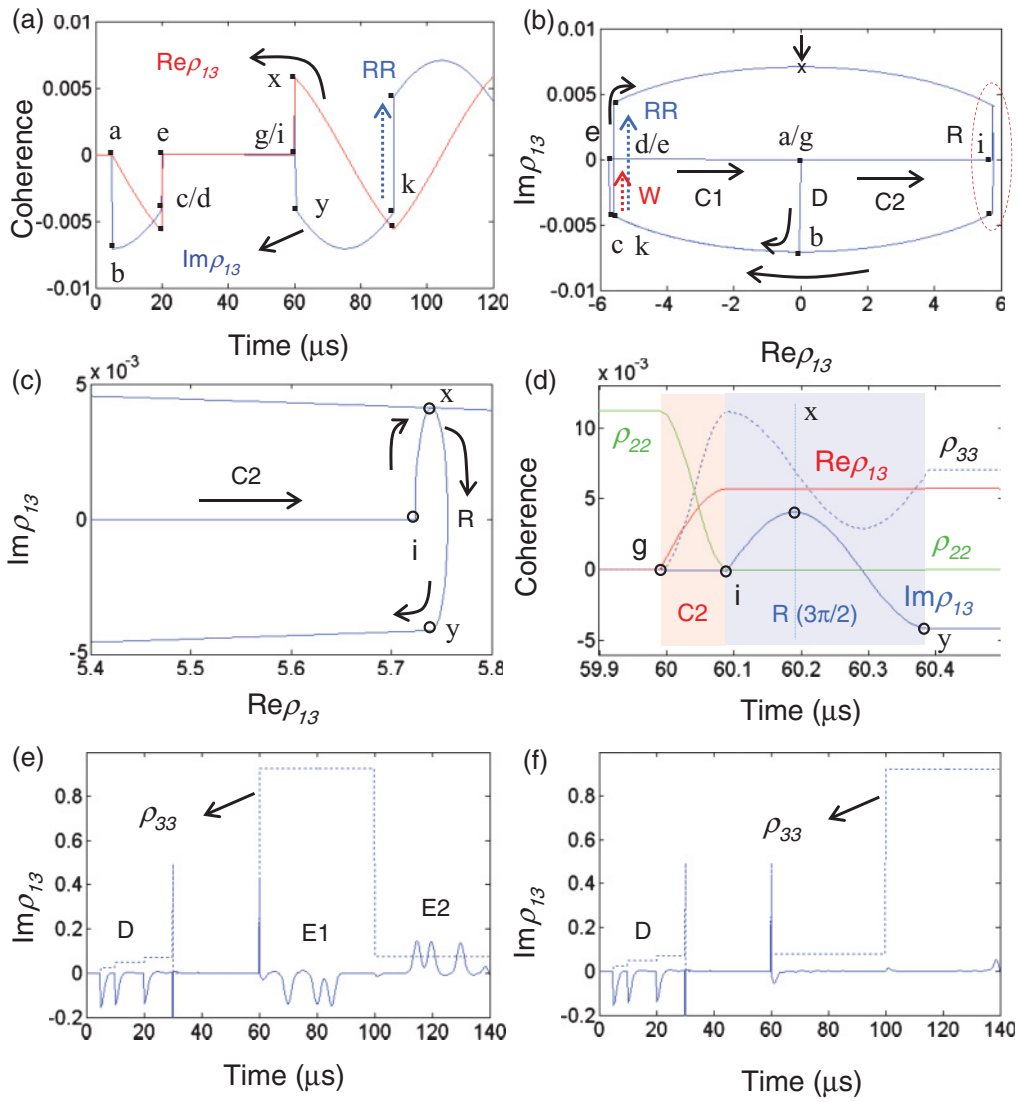

FIG. 4. (Color online) (a) Coherence evolution for $\delta = 10$ kHz. (b) Bloch vector description for (a). (c) and (d) Expanded features for the R interaction [see the red dotted circle in (b)]. (e) Three consecutive data pulse for (a). (f) For the first $\pi/2$ pulse area of R in (b).

final echo $E2$ is the same as that of the data pulses, which is a direct result of double rephasing. This normally ordered echo sequence gives a practical benefit to multimode photon information processing.

Figure 4(f) supports the phase recovery condition with $\pi/2$ R. As a result, there is no photon echo due to no rephasing, as discussed in Fig. 4(d). Echo $E2$ is also cancelled because of no $E1$. This phase recovery condition is very important in dealing with the optical locking pulses for storage time extension [10,12,15,16].

In conclusion, coherent atom phase control in a collective atom ensemble was studied for ultralong, inversion-free photon echoes. Storage time extension is due to the inherent property of phase locking in 3PE via optical-spin coherence transfer. Using optical phase locking, the transferred spin coherence becomes independent from spin dephasing, where the present scheme can be applied for ultralong quantum memories applicable to quantum repeaters in long-distance quantum communications.

This work was supported by the Creative Research Initiative Program (Grant No. 2011-0000433) of the Korean Ministry of Education, Science and Technology via the National Research Foundation.

[1] L. Jiang, J. M. Taylor, N. Khaneja, and M. D. Lukin, Proc. Natl. Acad. Sci. USA **104**, 17291 (2007), and references therein.

[2] W. Dür, H.-J. Briegel, and P. Zoller, in *Lectures on Quantum Information*, edited by D. Bruß (Wiley-VCH, Weinheim, 2010).

[3] N. A. Kurnit, I. D. Abella, and S. R. Hartmann, Phys. Rev. Lett. **13**, 567 (1964).
[4] T. W. Mossberg, Opt. Lett. **7**, 77 (1982).
[5] R. M. Macfarlane and R. M Shelby, in *Spectroscopy of Solids Containing Rare Earth Ions*, edited by A. Kaplyanskii and R. M. Macfarlene (North-Holland, Amsterdam, 1987).
[6] B. Hosseini, B. M. Sparkes, G. Hetet, J. J. Longdell, P. K. Lam, and B. C. Buchler, Nature (London) **461**, 241 (2009).
[7] C. Clausen, I. Usmani, R. Bussieres, N. Sangouard, M. Afzelius, H. De Riedmatten, and N. Gisin, Nature (London) **469**, 508 (2011).
[8] E. Saglamyurek, N. Sinclair, J. Jin, J. A. Slater, D. Oblak, F. Bussieres, M. George, R. Ricken, W. Sohler, and W. Tittel, Nature (London) **469**, 512 (2011).
[9] M. P. Hedges, J. J. Longdell, Y. Li, and J. J. Sellars, Nature (London) **465**, 1052 (2010).
[10] B. S. Ham, Opt. Exp. **18**, 1704 (2010).
[11] M. Afzelius, I. Usmani, A. Amari, B. Lauritzen, A. Walther, C. Simon, N. Sangouard, J. Minar, H. de Riedmatten, N. Gisin, and S. Kröll, Phys. Rev. Lett. **104**, 040503 (2010).
[12] J. Hahn and B. S. Ham, New J. Phys. **13**, 093011 (2011).
[13] B. S. Ham, e-print arXiv:1101.5480.
[14] V. Damon, M. Bonarota, A. Louchet-Chauvet, T. Chaneliere, and J.-L. Le Gouet, New J. Phys. **13**, 093031 (2011).
[15] B. S. Ham, New J. Phys. **14**, 013003 (2012).
[16] B. S. Ham, Nat. Photonics **3**, 518 (2009).
[17] N. Sangouard, C. Simon, J. Minar, M. Afzelius, T. Chaneliere, and N. Gisin, Phys. Rev. A **81**, 062333 (2010).